Check for updates

Received: 27 March 2023 | Revised: 29 May 2023 | Accepted: 19 June 2023

DOI: 10.1111/ppl.13963

ORIGINAL RESEARCH

Physiologia Plantarum

Methylome, transcriptome, and phenotype changes induced by temperature conditions experienced during sexual reproduction in *Fragaria vesca*

Yupeng Zhang[1,2] | Tuomas Toivainen[3] | Kathryn Mackenzie[3] | Igor Yakovlev[1] | Paal Krokene[1] | Timo Hytönen[3] | Paul E. Grini[2] | Carl Gunnar Fossdal[1]

[1]Department of Molecular Plant Biology, Norwegian Institute of Bioeconomy Research, Ås, Norway

[2]EVOGENE, Department of Biosciences, University of Oslo, Oslo, Norway

[3]Department of Agricultural Sciences, Viikki Plant Science Centre, University of Helsinki, Helsinki, Finland

Correspondence
Yupeng Zhang, Department of Molecular Plant Biology, Norwegian Institute of Bioeconomy Research, 1431 Ås, Norway.
Email: yupeng.zhang@nibio.no

Paul E. Grini, EVOGENE, Department of Biosciences, University of Oslo, 0313 Oslo, Norway.
Email: paul.grini@ibv.uio.no

Carl Gunnar Fossdal, Department of Molecular Plant Biology, Norwegian Institute of Bioeconomy Research, 1431 Ås, Norway.
Email: carl.gunnar.fossdal@nibio.no

Funding information
Norway Research Council, Grant/Award Number: 249958

Edited by S. Pelaz

Abstract

Temperature conditions experienced during embryogenesis and seed development may induce epigenetic changes that increase phenotypic variation in plants. Here we investigate if embryogenesis and seed development at two different temperatures (28 vs. 18°C) result in lasting phenotypic effects and DNA methylation changes in woodland strawberry (*Fragaria vesca*). Using five European ecotypes from Spain (ES12), Iceland (ICE2), Italy (IT4), and Norway (NOR2 and NOR29), we found statistically significant differences between plants from seeds produced at 18 or 28°C in three of four phenotypic features investigated under common garden conditions. This indicates the establishment of a temperature-induced epigenetic memory-like response during embryogenesis and seed development. The memory effect was significant in two ecotypes: in NOR2 flowering time, number of growth points and petiole length were affected, and in ES12 number of growth points was affected. This indicates that genetic differences between ecotypes in their epigenetic machinery, or other allelic differences, impact this type of plasticity. We observed statistically significant differences between ecotypes in DNA methylation marks in repetitive elements, pseudogenes, and genic elements. Leaf transcriptomes were also affected by embryonic temperature in an ecotype-specific manner. Although we observed significant and lasting phenotypic change in at least some ecotypes, there was considerable variation in DNA methylation between individual plants within each temperature treatment. This within-treatment variability in DNA methylation marks in *F. vesca* progeny may partly be a result of allelic redistribution from recombination during meiosis and subsequent epigenetic reprogramming during embryogenesis.

1 | INTRODUCTION

DNA methylation has recently been proposed to mediate local adaptation and responses to climate change in woodland strawberry (*Fragaria vesca* L.; Sammarco et al., 2022). Stable epigenetic variants with early flowering and late stolon production were observed in azacytidine-induced hypomethylated plants, and these variants were transmitted through meiosis (sexual reproduction; Xu et al. 2016a, 2016b). DNA methylation usually

This is an open access article under the terms of the Creative Commons Attribution-NonCommercial-NoDerivs License, which permits use and distribution in any medium, provided the original work is properly cited, the use is non-commercial and no modifications or adaptations are made.
© 2023 The Authors. *Physiologia Plantarum* published by John Wiley & Sons Ltd on behalf of Scandinavian Plant Physiology Society.

refers to the 5′-methylation of cytosine, which is the most common methylated base. High DNA methylation levels are usually associated with transposable elements and heterochromatin (Weber & Schübeler, 2007; Zhang et al., 2006). At the single gene level, increased methylation (hypermethylation) of promoter regions can suppress gene expression (Bird et al., 1985; Laurent et al., 2010).

DNA methylation occurs in three nucleotide contexts: two symmetric forms in the CGN and CHG contexts and one asymmetric form in the CHH context (where H is any base except G; Law & Jacobsen, 2010). The different DNA methylation contexts are mainly formed and maintained by three different types of methyltransferases: methyltransferase 1 (MET1) carries out CG (CGN) methylation, chromomethylase 3 affects CHG and CHH methylation, and domains rearranged methyltransferase 2 (DRM2) is another CHH methyltransferase (Cao et al., 2003; Lindroth et al., 2001; Pontes et al., 2006). In addition to these methyltransferases, plants have a unique RNA-directed DNA methylation (RdDM) machinery. RdDM needs RNA polymerase IV (POL IV) and RNA-dependent RNA polymerase 2 to generate small interfering RNA (siRNA) from double-stranded RNA. Methylation is then completed by POL V together with these siRNAs, ARGONAUTE 4/6, and DRM2 (Eun et al., 2012; Ji & Chen, 2012; Pikaard et al., 2012). Also unique to plants is the ability to effectively remove DNA methylation by exchanging methylated cytosines with unmethylated cytosines. The functional units affecting this demethylation are DNA glycosylases, of which *Arabidopsis thaliana* has four: repressor of silencing 1 (ROS1), Demeter, Demeter-like protein 2, and Demeter-like protein 3 (Agius et al., 2006; Gehring et al., 2006; Gong et al., 2002; Morales-Ruiz et al., 2006; Ortega-Galisteo et al., 2008; Penterman et al., 2007).

DNA methylation, histone modifications, and noncoding RNAs can be involved in forming an epigenetic memory that can be passed on to new cells (through mitosis) or new generations (through meiosis). In *A. thaliana*, the most well-studied epigenetic memory-like response to environmental temperature conditions is vernalization—the induction of flowering by exposure to prolonged low temperature (winter). Vernalization involves noncoding RNAs, DNA methylation, and altered histone modifications. The key module of vernalization is the flowering repressor flowering locus C (FLC). Several epigenetic mechanisms are involved in the regulatory network around FLC, including the histone modifications H3K27me3, H3K4me3, and H3K36me3, and the noncoding RNAs cold-induced long antisense intragenic RNA, cold assisted intronic noncoding RNA, and cold of winter-induced noncoding RNA from the promoter (Csorba et al., 2014; Heo & Sung, 2011; Jiang et al., 2009; Kim & Sung, 2017; Tavares et al., 2012; Yuan et al., 2016; Zhao et al., 2005). Another case of epigenetic memory found in *A. thaliana* is the effect of high osmotic stress that can be passed on to the next generation, mainly through the female gametes (Wibowo et al., 2016).

Epigenetic memory can be cell type- or organ-specific, and organ-specific epigenetic marks are known to be inherited through mitosis and possibly even through meiosis (Wibowo et al., 2018). Strong evidence for an epigenetic memory of environmental conditions also exists for gymnosperms, and this memory can be transmitted through both sexual and asexual propagation (Carneros et al., 2017; Yakovlev et al., 2012). Different temperature sums experienced during embryogenesis in Norway spruce (*Picea abies*) induce so-called epitypes with lasting, reproducible, and predictable changes in adaptive traits such as bud phenology and frost tolerance (Carneros et al., 2017). This temperature-induced epigenetic memory affects the timing of bud burst and bud set in different epitypes to a similar extent as that observed between ecotypes (Yakovlev et al., 2008). Transcriptomic reprogramming of genes involved in the epigenetic machinery, day length responses, bud phenology, and frost tolerance is observed between epitypes, and this epigenetic memory also involves the sRNA machinery and specific small RNAs (Carneros et al., 2017; Yakovlev et al., 2010).

Plants do not completely remove epigenetic marks during meiosis (Anastasiadi et al., 2021). Thus, plants may need to reset or modify epigenetic marks during gametogenesis or embryogenesis. For instance, the vernalized state in *A. thaliana* is epigenetically maintained in plants that can flower in the spring but is reset in the next generation. The epigenetic marks near *FLC* are reset during embryogenesis by competitive binding of leafy cotyledon 1, leafy cotyledon 2, and FUSCA3 to Polycomb repressive complex 2 recruitment sites, thus diluting repressive H3K27 marks during rapid cell divisions following fertilization (Tao et al., 2019). Also, FLC is reset during gametogenesis by removing H3K27me3-marked histone and replacing this with a sperm-specific histone (Borg et al., 2020; Finnegan & Dennis, 2007; Ingouff et al., 2010). Embryogenesis might thus be a developmental stage sensitive to external signals, such as environmental changes, that could affect the creation and erasure of epigenetic marks of importance for the resulting phenotype.

To study how temperature affects the phenology, transcriptome, and genomic methylation marks of plants, we used *F. vesca*. This perennial species is widely distributed across Eurasia and is already used as a model for the economically important Rosaceae family. *Fragaria vesca* is considered to be a distant ancestor of *Fragaria chiloensis* and *Fragaria virginiana*, the direct ancestors of the cultivated octoploid strawberry *Fragaria* × *ananassa* (Liston et al., 2014; Shulaev et al., 2008). *Fragaria vesca* is a good model for understanding the impacts of climate change in both short- and long-lived plants, as it is relatively long-lived but can reproduce asexually and sexually in a relatively short time.

We set up an experimental system to test for possible epigenetic memory effects in plants that experienced different temperature conditions during sexual propagation (i.e., during embryogenesis and seed development). We (1) examined if temperature had a lasting effect on major phenotypic traits scored under common garden conditions, (2) identified differentially methylated regions (DMRs) and differentially methylated genes (DMGs) in three methylation contexts, and (3) explored genes that were both differentially expressed and differentially methylated using genome-based expression profiling and focusing on genes related to flowering, gibberellin synthesis, epigenetic mechanisms, and transcription factor function.

2 | MATERIALS AND METHODS

2.1 | Plant materials and experimental conditions

We used clonal plants of five *Fragaria vesca* ecotypes (i.e., genotypes): "ES12" (43.5339°N, 6.5271°W, 138 m, Spain), "ICE2" (63.9988°N,

13993054, 2023, 4, Downloaded from https://onlinelibrary.wiley.com/doi/10.1111/ppl.13963 by University Of Oslo, Wiley Online Library on [12/01/2024]. See the Terms and Conditions (https://onlinelibrary.wiley.com/terms-and-conditions) on Wiley Online Library for rules of use; OA articles are governed by the applicable Creative Commons License

19.9604°W, 99 m, Iceland), "IT4" (46.2398°N, 11.2360°E, 949 m, Italy), "NOR2" (69.9395°N, 23.0964°E, 23 m, Norway), and "NOR29" (69.5302°N, 18.3808°E, 0 m, Norway). Plants were cultivated in growth chambers equipped with metal-halide lamps [160 μmol m^{-2} s^{-1} photosynthetically active radiation (PAR)] at 60%–65% humidity and fertilized weekly using a fertilizer solution (N–P–K: 17–4–25; Samad et al., 2017).

To produce seeds to test for temperature effects during sexual propagation, we self-pollinated flowers at 18°C and then kept plants at 18 or 28°C during embryogenesis and seed development. Following berry formation, we collected achenes produced at 18 or 28°C and germinated plants at 21°C on half-strength MS medium (Murashige & Skoog, 1962). Four weeks after germination, we transferred all seedlings to 400 mL pots and placed them under common-garden conditions in a climate chamber at 18°C and LD conditions (16/8 h light/dark). After another 4 weeks, we collected ∼20 mg of young unfolded leaf tissues for DNA methylation analysis and RNA sequencing. Tissues were collected from three randomly selected plants per ecotype 6 h after lights were turned on. One week later, all plants were moved to SD conditions (12/12 h) at 18°C for 6 weeks to induce flowering, as well as the number of growth points identified by having their own folded young leaves. After 1 week of SD conditions, we recorded the petiole length of the youngest fully developed leaf on each plant. Every second week for 18 weeks (6 weeks SD + 12 weeks LD), we recorded the number of runners formed and flowering time (as days to the first open flower).

2.2 | DNA and RNA isolation

Genomic DNA extraction from leaves was performed as described previously (Zeng et al., 2018). RNA isolation was performed following the instruction from Zeng et al. (2018) until the first step of chloroform extraction. The remainder of the isolation was performed using the Spectrum™ Plant Total RNA Kit (Sigma-Aldrich, STRN50) following the manufacturer's instructions. For each combination of ecotype and temperature, we extracted DNA/RNA from three independent biological replicates (individual plant samples), that is, a total of 30 samples (5 × 2 × 3).

2.3 | Bisulfite sequencing and RNA-sequencing

Bisulfite library preparation and sequencing were performed by BGI using the HiSeq platform. BGI also constructed transcriptome libraries and performed RNA-seq using the DNB-seq platform. After adding A-Tailing and Methylated Adapter, bisulfite DNA libraries were purified using the MiniElute PCR purification Kit (Cat. No. 28004, Qiagen) and bisulfite-treated using the Methylation-Gold kit (Zymo Research). Transcriptome libraries were prepared using BGI's protocol.

2.4 | Bioinformatics and statistical analyses

Three biological replicates of bisulfite reads were mapped and processed using methylpy (Schultz et al., 2016) with default parameters. Methylpy uses bowtie2 (Langmead & Salzberg, 2012) to align trimmed reads to the *F. vesca* reference genome (v4.0; Edger et al., 2018). In a de-duplication step, PCR duplicate reads were removed using MarkDuplicates (Picard2 suite v.2.18.1, https://github.com/broadinstitute/picard). Principal component analysis (PCA) and other analyses of global DNA methylation patterns and methylation of different ecotype and temperature combinations were done using methylpy and R with a 50 kb window size (Schultz et al., 2016). Global methylation circos plots were generated using shinyCircos with methylation data from the global methylation analysis data (Yu et al., 2018). Gene densities and methylation levels were plotted using the R program Rideogram (Hao et al., 2020). Statistical comparisons of methylation of different genomic features were made using the Wilcoxon test in R since this test does not require the data to be normally distributed. Differentially methylated regions (DMRs) for the CG, CHG, and CHH methylation contexts were detected using the DMRfind function of methylpy. Differentially methylated sites (DMSs) were identified using root mean square testing with a false discovery rate (FDR) of 0.003, 1000 permutations, and the chloroplast sequence as the unmethylated control. DMSs located within 250 bps were merged into a single DMR. Minimum read coverage of 30 and FDR 0.001 were used as the requirements for DMRs calling (Schultz et al., 2016). The methylation distribution pattern along genes and repetitive sequences was visualized using the R package methimpute (Taudt et al., 2018). To calculate the methylation degree, body portions of genes and repetitive elements (REs) were sectioned into 20 bins, while flanking areas (2 kb) were sectioned into 20 bins of 100 bp each. DMRs were mapped to genomic features using the R program ChIPseeker (Yu et al., 2015). DMR circos graphs were created and visualized using shinyCircos (Yu et al., 2018). Venn diagrams were constructed using bioinformatics.psb.ugent.be/webtools/Venn/. Gene Ontology (GO) enrichment analysis was performed using the clusterprofiler tool in R (Wu et al., 2021). Any positional impacts of REs were investigated using the Games–Howell test from the R package rstatix (https://cran.r-project.org/web/packages/rstatix/index.html). Heatmaps were generated using the pheatmap R package (https://cran.r-project.org/web/packages/pheatmap/index.html).

Three independent biological replicates of RNA-seq were processed using CLC Genomics Workbench's default settings (Qiagen Ltd). Volcano plots were generated using the ggplot2 package in R and the log2FoldChange and log10 *p* values from the CLC output. CLC Genomics Workbench uses trimmed mean of *M* values (TMM) for library size normalizations. A generalized linear model was used as a statistical model to call differentially expressed genes. The Wald test was used to determine differentially expressed genes. Statistical tests for differentially expressed genes (DEGs) were performed using the Wald tests (manual for CLC Genomics Workbench 21.0.2). Statistical assessment of overlapping DMGs and DEGs (i.e., differentially expressed and differentially methylated genes; DEDMGs), was done using Fisher's exact test (http://nemates.org/MA/progs/overlapstats.html). REs in DATASHEET1 were predicted using REPEATMODELER2 with default parameters, while pseudogenes (DATASHEET2) were predicted using pseudopipe (Flynn et al., 2020; Zhang et al., 2006).

13993054, 2023, 4, Downloaded from https://onlinelibrary.wiley.com/doi/10.1111/ppl.13963 by University Of Oslo, Wiley Online Library on [12/01/2024]. See the Terms and Conditions (https://onlinelibrary.wiley.com/terms-and-conditions) on Wiley Online Library for rules of use; OA articles are governed by the applicable Creative Commons License

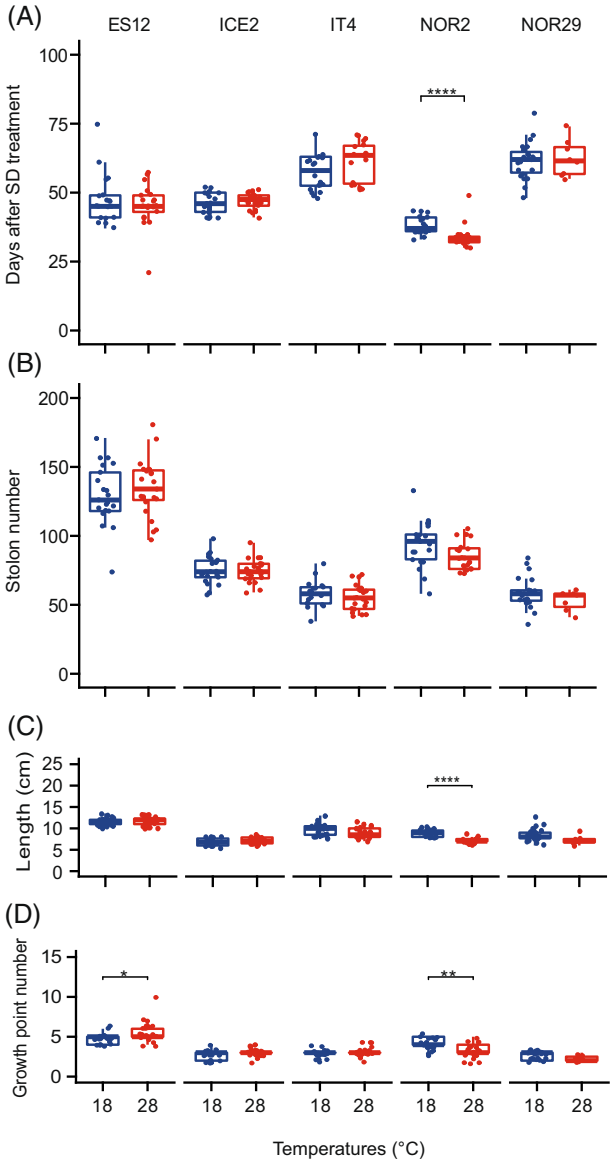

FIGURE 1 Phenotypic differences between *Fragaria vesca* plants germinated from seeds produced at 18 or 28°C. Phenotypes were scored under common-garden conditions after flower-inducing short-day (SD) treatment. Plots show flowering time (A), total number of stolons (B), petiole length (C), and number of growth points (D) in the ecotypes ES12, ICE2, IT4, NOR2, and NOR29. Flowering time was measured as days from the start of SD treatment until the first flower had opened completely. Flowering time in ES12 plants was measured after an additional 10°C treatment. Brackets and asterisks indicate significant differences calculated from Wilcoxon tests: *$0.01 \le p < 0.05$; **$0.001 \le p < 0.01$; ***$0.0001 \le p < 0.001$, ****$0.00001 \le p < 0.0001$. Box plots show median values ($n = 10$), the interquartile range (difference between the 75th and 25th percentiles), and 95% confidence intervals (error bars).

2.5 | Accession numbers and supplemental data

All sequences generated in this study are deposited in the National Center for Biotechnology Information Sequence Read Archive (https://www.ncbi.nlm.nih.gov/sra) under project number PRJNA882853. Data and Tables are available at GitHub (https://github.com/sherlock0088/FvSex).

3 | RESULTS

3.1 | Lasting impacts on phenotypic traits

To uncover any long-term phenotypic changes indicative of a temperature-induced epigenetic memory effect, we tested whether a 10°C difference experienced only during sexual reproduction generated lasting phenotypic alterations in the resulting plants. Using five European *Fragaria vesca* ecotypes, we generated seeds at 18 and 28°C. Seedlings that germinated from these seeds were propagated under common-garden conditions to investigate differences in flowering time, runner number, petiole length, and growth point number (Figure S1).

Flowering time was recorded as days to the first open flower that appeared after the start of flower-inducing short-day (SD) treatment. A significant difference in flowering time between temperature treatments was only found in the NOR2 ecotype (Figure 1A, Datasheet S1; Wilcoxon test: $0.05 > p > 0.0001$). The ES12 ecotype did not flower at all under the conditions used for the other ecotypes but had to be subjected to cold treatment (vernalization) to flower.

The number of stolons generated per plant was counted every second week for 10 consecutive time points over 18 weeks. The ES12 and NOR29 ecotypes produced the highest and lowest number of stolons, respectively (Figure 1B, Datasheet S1). Although stolon number varied between ecotypes, no significant differences between temperatures could be observed (Figure S2, Datasheet S1).

Petiole length and the number of growing points on each plant were measured 1 week after the start of SD treatment. ES12 had the longest petioles, while ICE2 had the shortest (Figure 1C, Datasheet S1). A significant temperature effect was found only in NOR2, where plants from seeds generated at 28°C had significantly shorter petioles than plants from seeds generated at 18°C (Figure 1C, Datasheet S1; Wilcoxon test, $0.05 > p > 0.0001$). The number of growing points differed significantly between temperature treatments in ecotype ES12 and NOR2, and these ecotypes also had the largest number of growing points (Figure 1D, Datasheet S1; Wilcoxon test, $0.05 > p > 0.0001$).

In summary, we observed statistically significant effects for three of the four phenotypic features investigated under common-garden conditions, indicating that a memory effect was induced by the temperature conditions experienced during embryogenesis and seed development. Phenotypic differences between plants germinated from seeds produced at 18 versus 28°C were most pronounced in the NOR2 ecotype.

3.2 | DNA methylation in plants that experienced seed development at 18°C

We sequenced bisulfite-treated genomic DNA from leaves of five *F. vesca* ecotypes grown from the seeds generated at 18 or 28°C.

13993054, 2023, 4, Downloaded from https://onlinelibrary.wiley.com/doi/10.1111/ppl.13963 by University Of Oslo, Wiley Online Library on [12/01/2024]. See the Terms and Conditions (https://onlinelibrary.wiley.com/terms-and-conditions) on Wiley Online Library for rules of use; OA articles are governed by the applicable Creative Commons License

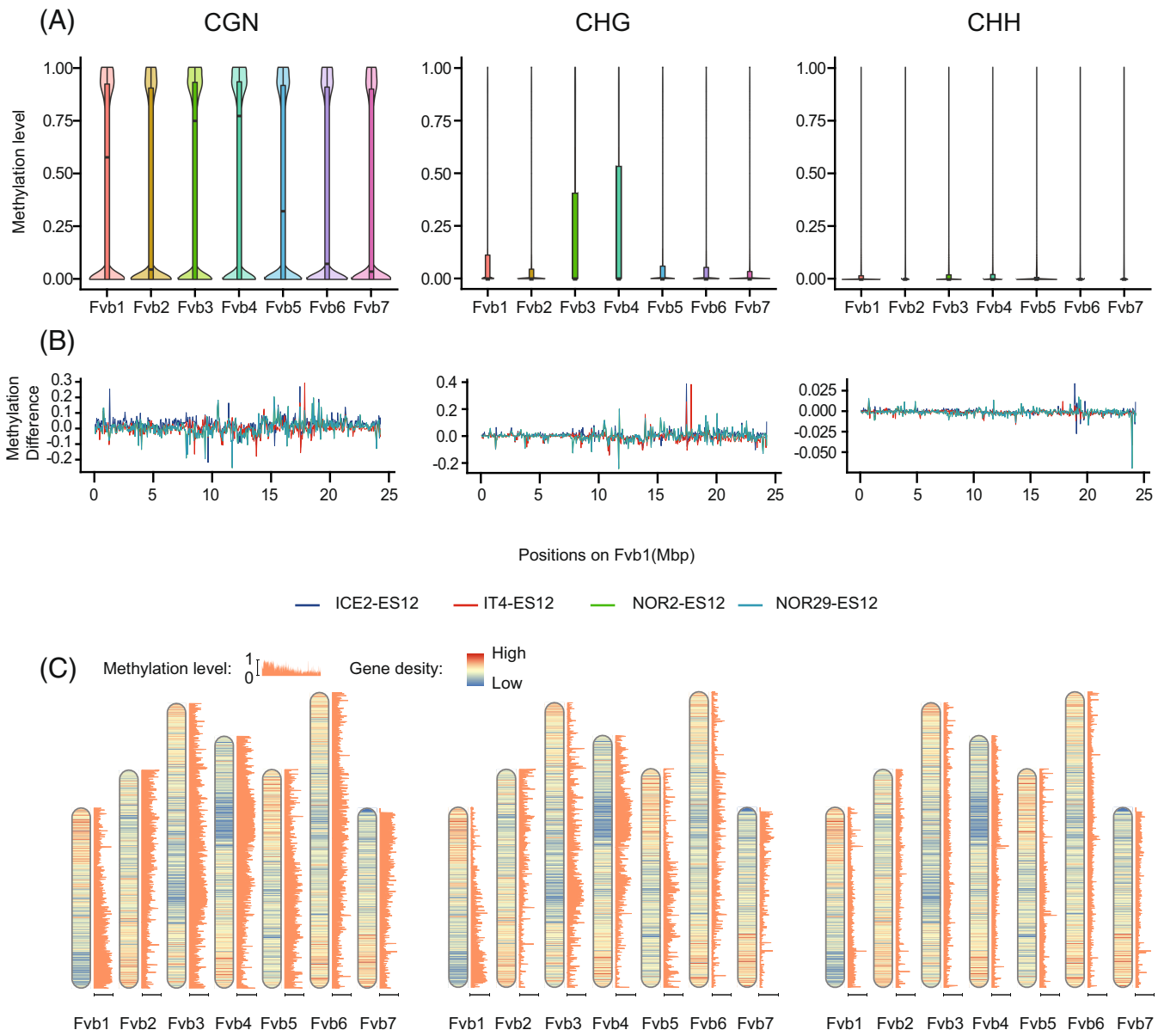

FIGURE 2 DNA methylation and gene density in leaves of *Fragaria vesca* ecotypes gone through seed development at 18°C. Average methylation level (methylated reads/total reads, using a 50 kb window) was calculated based on the methylation level of each methylated site, discarding any unmethylated sites. All methylation data show the CGN, CHG, and CHH methylation contexts (where N is any base and H is any base other than G). (A) Violin plots of methylation level for all seven *F. vesca* (Fv) chromosomes in the NOR2 ecotype. Plots show the median (horizontal black line, $n = 3$), the 25th and 75th percentiles (colored bars), and 95% confidence intervals (error bars). (B) Methylation differences between *F. vesca* ecotypes ES12 (Spain; baseline), ICE2 (Iceland), IT4 (Italy), NOR2 (Norway), and NOR29 (Norway) along chromosome Fvb1. (C) Comparison of methylation level and gene density along all seven *F. vesca* chromosomes in the NOR2 ecotype.

All the resulting plants were grown and sampled at a common-garden environment temperature to discover lasting effects of the seed temperature conditions experienced (Figure S1). After quality control, we obtained an overall coverage of >20× per replicate and achieved comparable mapping rates for all ecotypes (Datasheet S2).

We first compared global cytosine methylation in the CGN, CHG, and CHH context at 18°C to investigate methylation differences and similarities between the five ecotypes. The symmetric CGN context had the highest methylation degree of the three contexts (Figure 2A). Out of 8 million CGN sites identified in the *F. vesca* genome, 48%–54% were methylated in the different ecotypes (Datasheet S2). In comparison, the average methylation levels of CHG and CHH sites were ∼19% to ∼24% and ∼2% to ∼4%, respectively (Datasheet S2). Although individual chromosomes showed distinct methylation patterns, all ecotypes displayed analogous methylation patterns across chromosomes (Figures 2A, S3, and S4). Thus, there were methylation differences between ecotypes grown under the same temperature conditions (Figures 2B and S5, Datasheet S3). The ICE2 ecotype was overall hypermethylated

13993054, 2023, 4, Downloaded from https://onlinelibrary.wiley.com/doi/10.1111/ppl.13963 by University Of Oslo, Wiley Online Library on [12/01/2024]. See the Terms and Conditions (https://onlinelibrary.wiley.com/terms-and-conditions) on Wiley Online Library for rules of use; OA articles are governed by the applicable Creative Commons License

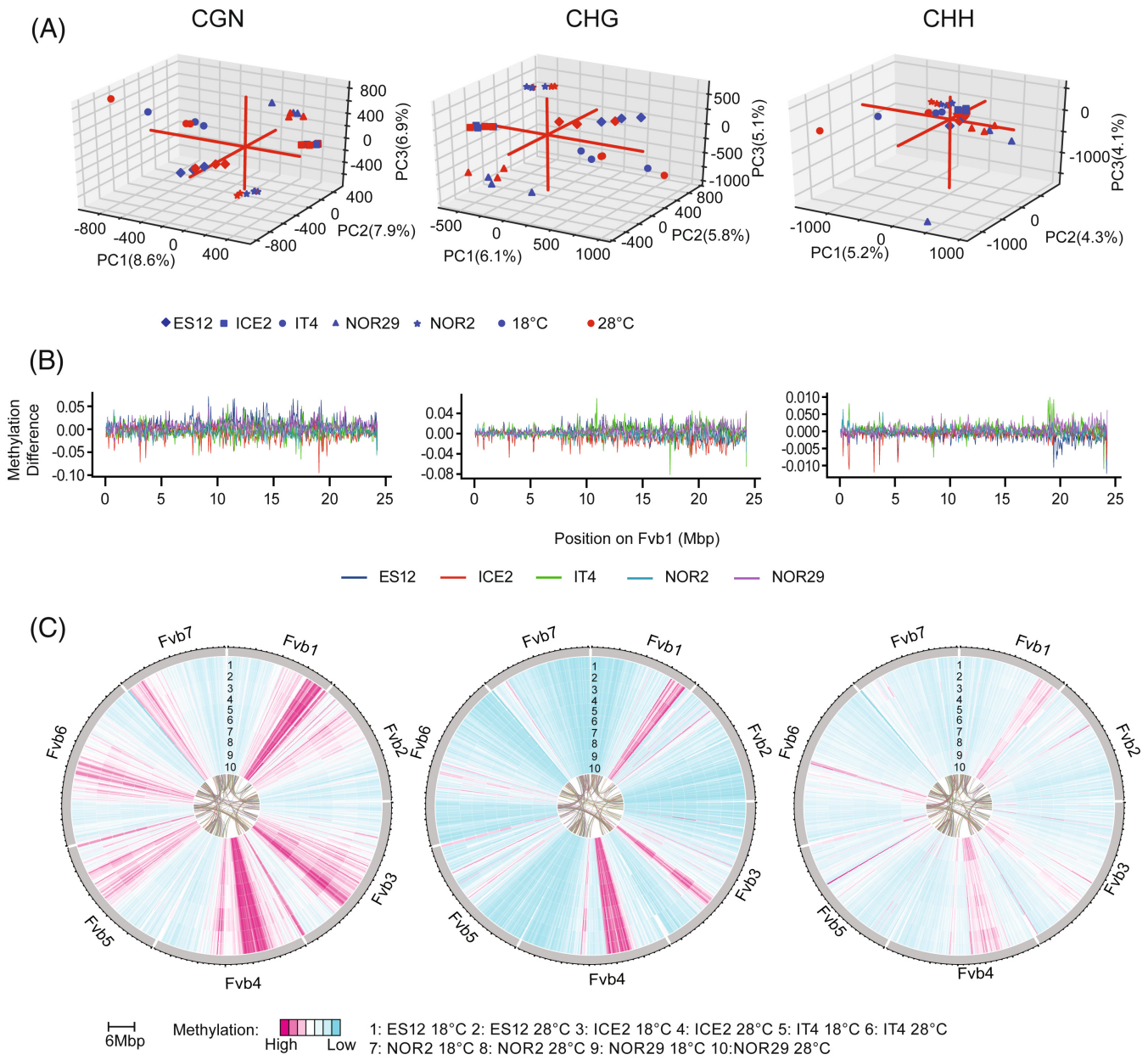

FIGURE 3 DNA methylation in leaves of five *Fragaria vesca* ecotypes gone through seed development at 18 or 28°C). Ecotypes are from Spain (ES12), Iceland (ICE2), Italy (IT4), and Norway (NOR2, NOR29). All methylation data show the CGN, CHG, and CHH methylation contexts (where N can be any base and H can be any base other than G). Three biological replicates were used for each ecotype-temperature combination. (A) Principal component analysis of methylation level (methylated reads/total reads) in ecotypes germinated from seeds produced at 18°C (blue symbols) or 28°C (red symbols). Red lines indicate the *x*, *y*, and *z* axes. (B) Methylation differences between temperatures (28 vs. 18°C) on *F. vesca* chromosome 1 (Fvb1) in the different ecotypes. Methylation differences were calculated for each methylation context separately, using a 50 kb window and 18°C as a reference. (C) Methylation patterns along all seven *F. vesca* chromosomes for all ecotypes and both temperatures, using a 50 kb window. Lanes 1–10 show methylation levels for each ecotype-temperature combination. Connecting lines in the middle indicate coding regions (CDS) that showed synteny.

compared to all other ecotypes, regardless of whether the comparison was made at the single-chromosome or whole-genome level (Figures 2B and S5, Datasheet S3). Chromosome regions with high methylation density corresponded to regions with low gene density and centromeric heterochromatin (Qu et al., 2017; Figures 2C and S6).

3.3 | Lasting temperature-induced changes in global DNA methylation

Principal component analysis (PCA) of methylation profile differences in plants from seeds that had experienced 18 or 28°C revealed some variation between biological replicates (Figure 3A). The analysis

13993054, 2023, 4, Downloaded from https://onlinelibrary.wiley.com/doi/10.1111/ppl.13963 by University Of Oslo, Wiley Online Library on [12/01/2024]. See the Terms and Conditions (https://onlinelibrary.wiley.com/terms-and-conditions) on Wiley Online Library for rules of use; OA articles are governed by the applicable Creative Commons License

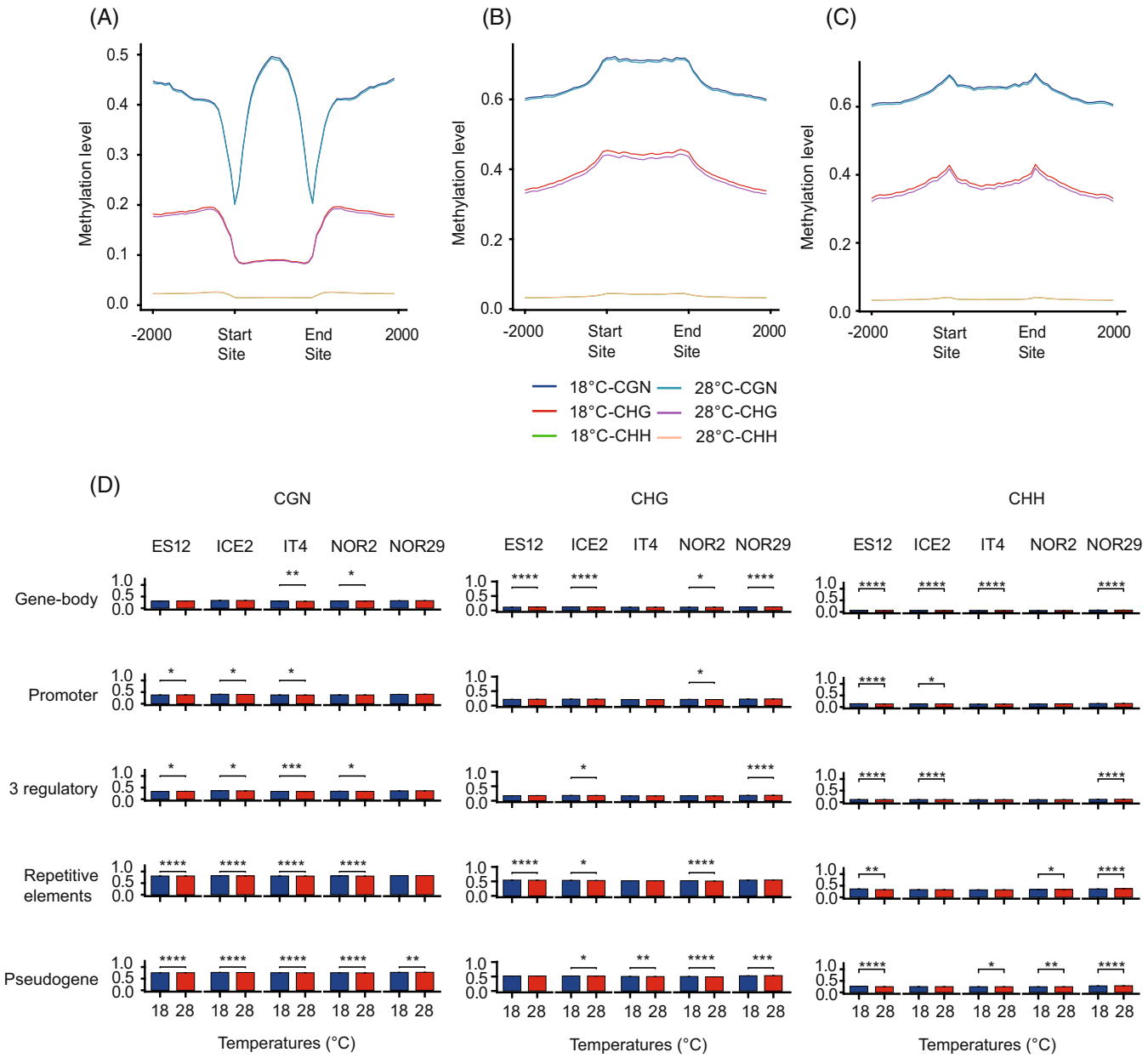

FIGURE 4 DNA methylation of protein-coding genes, repetitive elements, and pseudogenes in leaves of *Fragaria vesca* ecotypes gone through seed development at 18 or 28°C. Methylation level along protein-coding genes (A), repetitive elements (B), and pseudogenes (C) for different methylation contexts (CGN, CHG, and CHH, where N can be any base and H can be any base other than G) in the NOR2 ecotype. Each genomic feature and regions 2 kb upstream and downstream of these were divided into 20 pieces to calculate methylation levels (methylated reads/total reads, using a 50 kb window). Colored lines show different combinations of temperature and methylation contexts. (D) Average methylation level for different genomic features in five *F. vesca* ecotypes (ES12, ICE2, IT4, NOR2, and NOR29) for different methylation contexts and temperature conditions. Read counts from three plants were merged for genic elements ($N = 34{,}009$), repetitive elements ($N = 71{,}885$), and pseudogenes ($N = 55{,}593$). Asterisks indicate significant differences: *$0.01 \le p < 0.05$; **$0.001 \le p < 0.01$; ***$0.0001 \le p < 0.001$; ****$0.00001 \le p < 0.0001$. Error bars show 95% confidence intervals.

further highlighted differences in methylation patterns between ecotypes, regardless of temperature treatment. Ecotype-specific differences were particularly prominent in the CGN and CHG contexts (Figure 3A). According to the PCA, these methylation contexts also differed between the temperatures experienced (Figure 3A). The lasting effect of elevated temperature treatment (28°C) on DNA methylation varied within and between ecotypes (Figure 3A, Datasheet S4).

At the chromosome level, we observed minor methylation changes in response to temperature treatment in the CGN, CHG, and CHH contexts for all ecotypes when using a 50 kb window resolution (Figures 3B and S7). All ecotypes showed ~1% methylation level change between 18 and 28°C for all methylation contexts (Datasheet S4). We made chromosome heat maps to compare the methylation level between ecotypes in more detail. These revealed ecotype-

13993054, 2023, 4, Downloaded from https://onlinelibrary.wiley.com/doi/10.1111/ppl.13963 by University Of Oslo, Wiley Online Library on [12/01/2024]. See the Terms and Conditions (https://onlinelibrary.wiley.com/terms-and-conditions) on Wiley Online Library for rules of use; OA articles are governed by the applicable Creative Commons License

specific hypo- and hypermethylated regions at 18 versus 28°C, but few chromosome regions showed temperature-specific methylation patterns within ecotypes (Figures 3C and S7). For the CHH methylation context, we observed temperature-related methylation changes in a few positions on different chromosomes at this level of resolution, while for the CGN and CHG contexts, hypo- and hypermethylated areas were largely shared between ecotypes irrespective of temperature treatment (Figures 3C and S7).

3.4 | Methylation changes in genic features

To determine the spatial association between DNA methylation and genes as well as REs, we calculated DNA methylation patterns along these genomic features and 2 kb upstream and downstream of them. For all genic methylation contexts, methylation levels were, as expected, lowest around the transcription start site (TSS) and transcription termination site (TTS; Figures 4A and S8; Edger et al., 2018; Liu et al., 2022). For REs, we observed a plateau of hypermethylation over the RE body region, flanked by regions with decreasing methylation levels for all methylation contexts (Figures 4B and S8). For pseudogenes, methylation peaked around the transcription start and termination sites and was lower within the body region (Figures 4C and S8). In plants from seeds exposed to elevated temperature, methylation levels dropped slightly in all regions analyzed. This was true for all methylation contexts in genes, REs, and pseudogenes (Figures 4A–C and S8).

To investigate the statistical significance of the lasting temperature-induced methylation changes, we analyzed global methylation differences between different genic regions, repetitive regions, and pseudogenes. On average, methylation levels in the CGN context were ~30%, 40%, and 35% for the promoter, gene-body, and 3′-prime region, respectively. The average CGN methylation level for repetitive regions and pseudogenes was considerably higher, with ~80% and 75%, respectively (Datasheet S5). All ecotypes displayed significant differences in four or more categories for these genic features when all methylation contexts were considered. However, except for CGN in IT4, no ecotype showed significant differences between temperatures for all genic features or all methylation contexts. For REs, we observed one or more, and for pseudogenes, two or more significant differences when all methylation contexts were considered (Figures 4D and S8, Datasheet S5). Notably, only the NOR2 ecotype showed significant differences in REs and pseudogenes between plants from seeds that had experienced the two contrasting temperatures for all methylation contexts. For CGN methylation change, the different ecotypes were quite similar with respect to both REs and pseudogenes, except for REs in NOR29 that lacked significant difference (Figures 4D and S8, Datasheet S5).

3.5 | DMRs are more common in the CGN than in the CHG or CHH contexts

We identified differentially methylated regions (DMRs) between treatments across all chromosomes for all ecotypes (Figures 5A and S9, Datasheet S6). The number of DMRs in the different methylation contexts varied between ecotypes, but most DMRs were in the CGN context (2456–7403 DMRs in the different ecotypes). The number of DMRs was lower in the CHG context (275–896 across ecotypes) and very low in the CHH context (67–152; Datasheet S6). The ICE2 ecotype had the greatest number of DMRs across all contexts. When we separated DMRs into hyper- and hypomethylated DMRs, we observed a similar proportion of hyper- and hypomethylated DMRs for all ecotypes and methylation contexts (Datasheet S6). When we matched DMRs to genes and intergenic regions, we found that >80% of CGN DMRs were located in genes and flanking regulatory regions (Figure 5B). This distribution between genic versus distal intergenic regions was not evident for CHG and CHH DMRs. Moreover, the distribution of DMRs within and close to genes (5′-UTR, promoter, exons, introns, 3′-UTR, and intergenic regions) was unique for each ecotype, with the CHH context having the largest distribution difference between ecotypes (Figure 5B, C). Over 50% of CGN DMRs were located in the 3′ direction, with most of them situated within 3 kb of the TSS. For CHG and CHH DMRs, the distribution was even between the 5′ and 3′ direction of TSS. However, an extreme deviation from this pattern was observed in NOR2, where CHH DMRs were heavily overrepresented in the 5′ direction of TSS (Figures 5C and S9).

3.6 | Ecotypes share genes that are differentially methylated in the CGN context

We define differentially methylated genes (DMGs) as genes with lasting temperature-induced DMRs in their promoter region (2 kb upstream to TSS) and/or gene body (between TSS and TTS). The number of DMGs was not evenly distributed among the three methylation contexts, with most DMGs being in the CGN context (in a manner similar to that observed for DMRs) (Datasheet S7). Each ecotype had its own unique set (>1144) of DMGs between treatments (Datasheet S7). When comparing DMGs shared between ecotypes, we found that the 19 DMGs common to all ecotypes were all methylated in the CGN context (Figure 6A). A much higher number of DMGs were shared between two or more ecotypes, most of which were in the CGN context (there were 63, 144, and 512 CGN DMGs shared by four, three, and two ecotypes, respectively). The number of shared DMGs was very modest in the CHG context and almost zero in the CHH context (5, 10, and 101 CHG DMGs and 0, 0, and 3 CHH DMGs were shared by four, three, and two ecotypes, respectively).

3.7 | Differentially expressed and differentially methylated genes are ecotype-specific

To identify genes that were both differentially expressed and differentially methylated, we performed a differential gene expression analysis of leaves sampled from plants at common garden conditions from seeds that had experienced 18 and 28°C and compared this with our

13993054, 2023, 4, Downloaded from https://onlinelibrary.wiley.com/doi/10.1111/ppl.13963 by University Of Oslo, Wiley Online Library on [12/01/2024]. See the Terms and Conditions (https://onlinelibrary.wiley.com/terms-and-conditions) on Wiley Online Library for rules of use; OA articles are governed by the applicable Creative Commons License

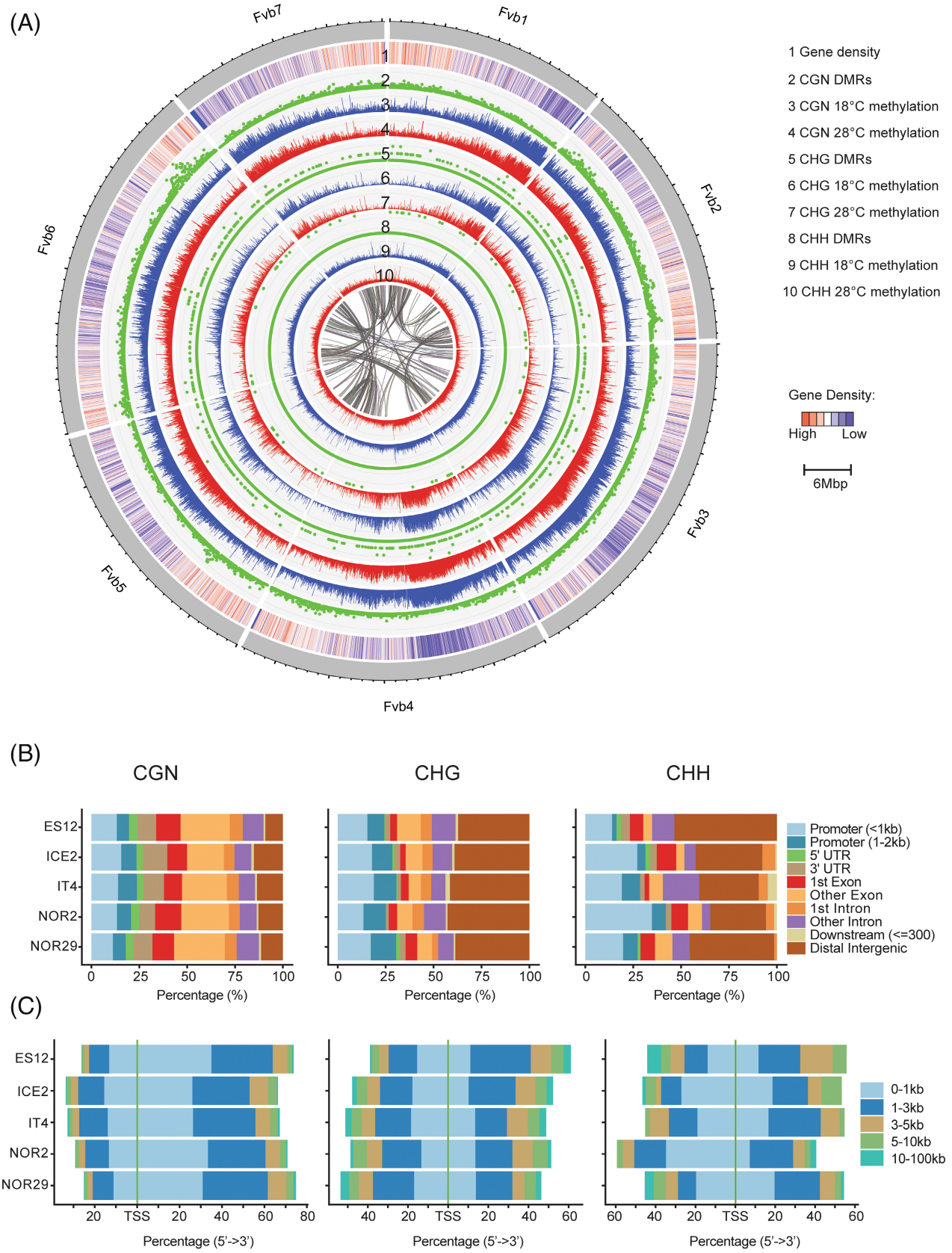

FIGURE 5 Legend on next page.

13993054, 2023, 4, Downloaded from https://onlinelibrary.wiley.com/doi/10.1111/ppl.13963 by University Of Oslo, Wiley Online Library on [12/01/2024]. See the Terms and Conditions (https://onlinelibrary.wiley.com/terms-and-conditions) on Wiley Online Library for rules of use; OA articles are governed by the applicable Creative Commons License

DNA methylation studies (Figures 6B and S10). Differentially expressed and differentially methylated genes (DEDMGs) were identified in all ecotypes and comprised 4% and 25% of all DEGs (Figure 6C, Datasheet S8). The number of DEDMGs in different ecotypes ranged from 9 to 103. The DEDMGs were ecotype-specific, with no DEDMGs being shared by all five ecotypes (Figure 6D). DEDMGs in individual ecotypes were enriched for several GO term categories, but none were shared by all the ecotypes (Datasheet S9). However, GO terms related to chromatin binding (GO:0003682) were shared by ICE2 and NOR2. When we correlated the gain or loss of CGN methylation with observed expression change, most DEDMGs were found to be downregulated, regardless of whether there was a gain or loss of methylation. Similarly, methylation gains or losses were also detected for upregulated genes but affected a smaller proportion of the DEDMGs (Figure 6E).

3.8 | REs located near genes may play an important role in gene regulation

REs are well-known targets of methylation, and RE methylation may influence the expression of nearby genes (Hirsch & Springer, 2017; Hollister & Gaut, 2009; Wang et al., 2013). We, therefore, examined the DNA methylation status of REs in the *F. vesca* genome, starting with general differences in RE methylation (DMR) between the two treatments (Figure 7A). For all methylation contexts, we observed both hypo- and hypermethylation at the 28 versus 18°C treatment, although the number of changes was low in the CHG context and very low in the CHH context. However, the level and direction of change differed noticeably between ecotypes for these two methylation contexts. NOR2 showed the most hypomethylation in plants derived from the 28°C seeds in the CHG context, while ES12 had notable hypomethylation in the CHH context. Conversely, IT4 and NOR29 had hypermethylation in 28°C treatment in the CHH context (Figure 7A).

To determine if methylation of REs was associated with the expression of nearby genes, we classified genes into four classes based on the distance between the gene and the closest RE: (1) genes with no RE within 10 kbp, (2) genes with a RE within 2 kbp, (3) genes with a RE within 2–5 kbp, and (4) genes with a RE within 5–10 kbp. Only REs that were less than 2 kbp from genes had a significant positional association with transcription (Games–Howell test, $0.05 > p \geq 0.000322$; Figures 7B and S11A). This association was observed across all ecotypes, and the most proximal REs consistently led to a reduction in gene expression. (Figures 7B and S11A). With respect to the effect of treatment, we saw a significant increase in gene expression change in plants from seeds having experienced 28 versus 18°C up to a distance of 2–5 kbp from the RE, but, to our surprise, not at 2 kbp or beyond 5 kbp (Games–Howell test, $0.05 > p$-value ≥ 0.027; Figure 7C, Datasheet S10, Figure S11B).

4 | DISCUSSION

Here we investigated possible connections between temperature conditions during sexual reproduction and epigenetic memory in *Fragaria vesca*. By exploring the whole-genome methylomes and transcriptomes of five ecotypes from Spain, Italy, Iceland, and northern Norway, we revealed DNA methylation changes and their putative effects on gene expression, paying particular attention to effects with lasting adaptive changes. We observed significant differences between plants from seeds produced at 18 versus 28°C in three of four phenotypic features when investigated under identical conditions. This indicates an epigenetic memory-like response during embryogenesis and seed development. The memory effect was significant in ecotype NOR2 for flowering time, number of growth points, and petiole length, and in ecotype ES12 for the number of growth points.

It has been proposed that population history influences methylomes more than short-term environmental changes and that *F. vesca* can increase phenotypic variation through methylome changes (de Kort et al., 2020). DNA methylation has also been suggested to mediate local adaptation and response to climate change in *F. vesca* (Sammarco et al., 2022). We used whole genome bisulfite sequencing to probe the methylome of our *F. vesca* ecotypes. During normal temperature conditions (18°C), there were ecotype-specific methylation differences over all chromosomes. The ecotypes ICE2 and NOR29 were generally hypermethylated, and NOR2 was hypomethylated compared to the ES12 and IT4 ecotypes. Unique hyper- and hypomethylated peaks occurred in all ecotypes when studied using a 50 kb resolution window. More differences were evident when we used a single nucleotide resolution, indicating that ecotypes have numerous specific as well as global methylation differences. These methylome differences between *F. vesca* ecotypes are likely related to differences in life history and population history, but it is difficult to assess how they impact the phenotype under normal, in situ conditions (i.e., possible phenotypic effects of methylation variants must be tested under common garden conditions). Most likely, the phenotypic

FIGURE 5 Chromosomal and genic distribution patterns of differentially methylated regions (DMRs) in leaves of *Fragaria vesca* ecotypes gone through seed development at 18 or 28°C. (A) Pattern of DMRs along all seven *F. vesca* (Fv) chromosomes in the NOR2 ecotype. Lane 1 shows gene density and lanes 2–10 show DMR density and methylation level (methylated reads/total reads; %) for different combinations of temperature and methylation context (CGN, CHG, or CHH, where N can be any base and H can be any base other than G). Connecting lines in the middle indicate coding regions (CDS) that showed synteny. (B) Distribution of DMRs for different methylation contexts across different genomic features in five *F. vesca* ecotypes. (C) Distribution of DMRs for different methylation contexts according to their distance (5′–3′ direction) from transcription start sites (TSS) in the different ecotypes. Three biological replicates (plants) were used for each ecotype and temperature combination.

13993054, 2023, 4, Downloaded from https://onlinelibrary.wiley.com/doi/10.1111/ppl.13963 by University Of Oslo, Wiley Online Library on [12/01/2024]. See the Terms and Conditions (https://onlinelibrary.wiley.com/terms-and-conditions) on Wiley Online Library for rules of use; OA articles are governed by the applicable Creative Commons License

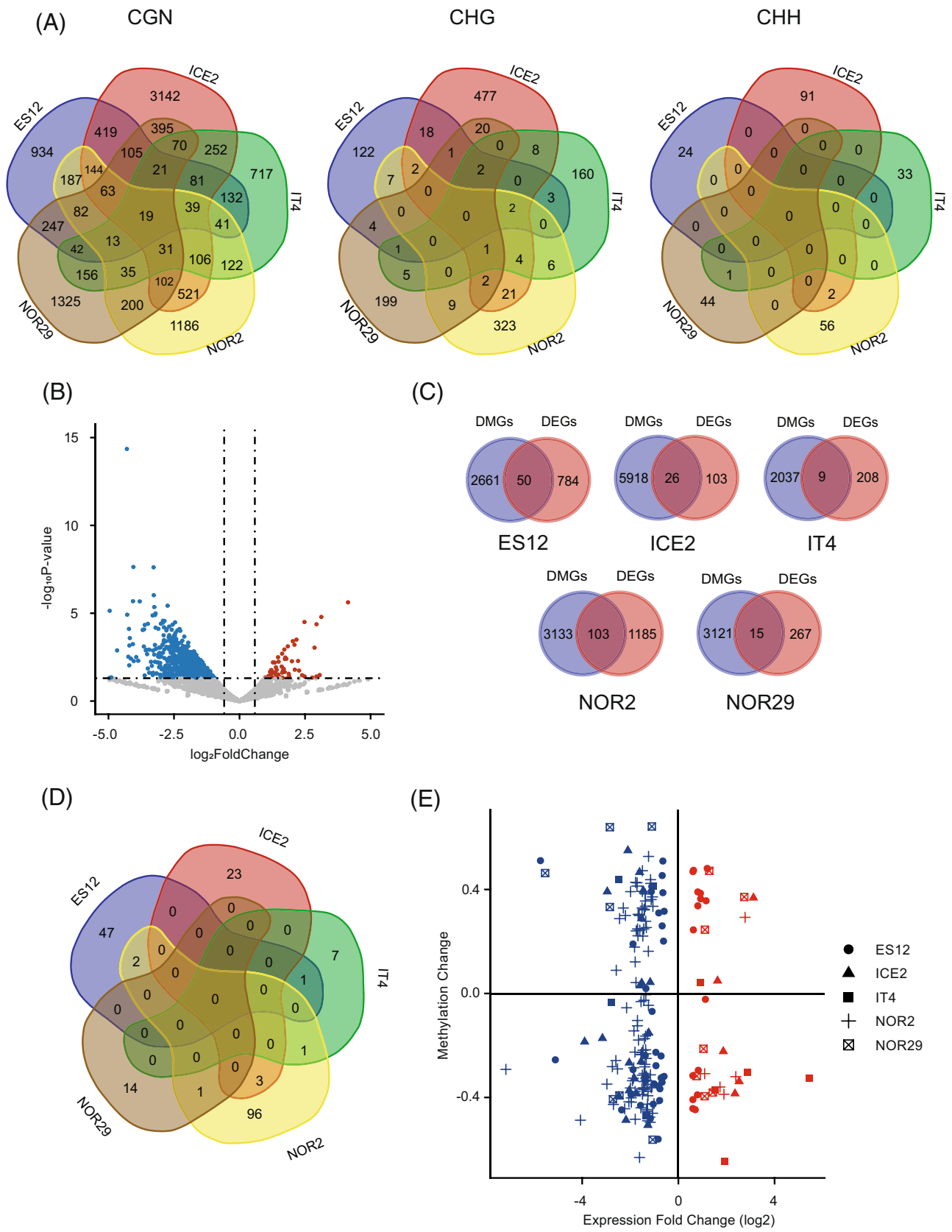

FIGURE 6 Legend on next page.

13993054, 2023, 4, Downloaded from https://onlinelibrary.wiley.com/doi/10.1111/ppl.13963 by University Of Oslo, Wiley Online Library on [12/01/2024]. See the Terms and Conditions (https://onlinelibrary.wiley.com/terms-and-conditions) on Wiley Online Library for rules of use; OA articles are governed by the applicable Creative Commons License

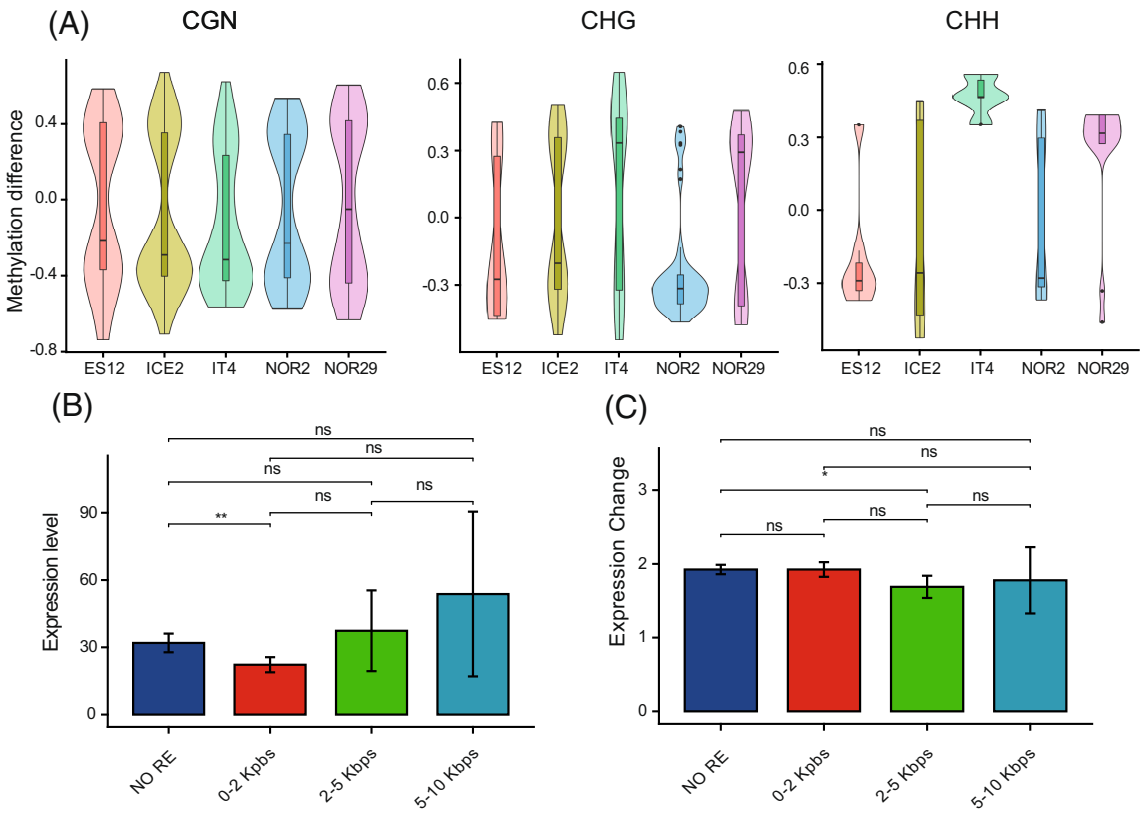

FIGURE 7 DNA methylation of repetitive elements (REs) and gene expression in leaves of *Fragaria vesca* ecotypes gone through seed development at 18 or 28°C. (A) Violin plots showing methylation change (at 28 vs. 18°C) in REs in different ecotypes (ES12, ICE2, IT4, NOR2, NOR29) for the CGN, CHG, and CHH methylation contexts (where N can be any base and H can be any base other than G). The average methylation value in differentially methylated regions was calculated based on the methylation level of each methylated site, discarding any unmethylated sites (methylated reads/total reads). Plots show the median (horizontal black line, $n = 3$), the 25th and 75th percentiles (colored bars), outliers (black circles), and 95% confidence intervals (error bars). (B, C) Positional relationship between REs and gene expression level (B) and absolute gene expression change (C) in ecotype NOR2 plants germinated from seeds produced at 28 versus 18°C. The distance from the gene to the nearest RE is given on the *x*-axis in kilobase-pairs (kbp). Asterisks indicate significant differences calculated by the Games–Howell test: *$0.01 \le p < 0.05$; **$0.001 \le p < 0.01$; ns = not significant. Error bars show 95% confidence intervals. Three biological replicates were used for each ecotype and temperature combination.

differences we observed in, for example, flowering time between ecotypes that were sexually propagated at identical temperature conditions were primarily linked to genetic differences.

We found that in plants grown under common garden conditions, the methylomes of *F. vesca* ecotypes were significantly altered by the elevated temperature experienced earlier during sexual reproduction. DNA methylation patterns have previously been studied in hypomethylated *F. vesca* using methylation-sensitive isoschizomers to detect methylation at CGN, CHG, and CHH contexts in two early-flowering lines of the ecotype Hawaii-4 (Xu et al. 2016a, 2016b). These studies found maintenance of DNA methylation at CGN and CHG sites across sexual generations and suggest that the early-flowering phenotype might be a result of methylation changes at these sites. Using whole-genome studies, we also found that most DNA methylation changes induced during sexual propagation were in the CGN and CHG contexts for five European *F. vesca* ecotypes. We identified a wide range of DMRs in all three methylation contexts, with CGN methylation being by far the most commonly changed

FIGURE 6 DNA methylation and gene expression in leaves of *Fragaria vesca* ecotypes gone through seed development at 18 or 28°C. (A) Venn diagrams showing numbers of differentially methylated genes (DMGs) for different ecotypes (ES12, ICE2, IT4, NOR2, NOR29) and methylation contexts (CGN, CHG, CHH, where N can be any base and H can be any base other than G). (B) Volcano plot showing differentially expressed genes (DEGs) in NOR2 plants propagated at 28 versus 18°C. Blue and red dots show downregulated and upregulated genes, respectively. Dashed lines delineate *p*-value ≤ 0.05 and |FoldChange| ≥ 1.5 calculated from three biological replicates. (C) Venn diagrams showing overlap between DEGs and DMGs in the different ecotypes. (D) Venn diagrams showing numbers of differentially expressed and differentially methylated genes (DEDMGs) in all ecotypes. (E) Scatter plot showing relationship between methylation change and expression change for all DEDMGs. Colors indicate direction of gene expression change (red: upregulated; blue: downregulated). Symbols indicate ecotypes.

13993054, 2023, 4, Downloaded from https://onlinelibrary.wiley.com/doi/10.1111/ppl.13963 by University Of Oslo, Wiley Online Library on [12/01/2024]. See the Terms and Conditions (https://onlinelibrary.wiley.com/terms-and-conditions) on Wiley Online Library for rules of use; OA articles are governed by the applicable Creative Commons License

context. In total, we called ∼2100 to ∼5900 differentially methylated genes (DMGs), mostly in the CGN context. The ecotype ICE2 had the highest number of DMGs, correlating with the observation that ICE2 displayed the strongest DNA methylation response to treatment. Overall, we found that the identified DMGs were predominantly ecotype-specific, as only a few induced methylation changes (DMRs or DMGs) were shared between ecotypes. This ecotypic-specific effect is in line with the observation that the lasting memory of the temperature treatment experienced during embryogenesis and seed development on flowering time, number of growth points, and petiole length also differed between the resulting progenies.

The fact that we found many more DMRs in the CGN context than in other methylation contexts points toward DNA methylation mediated by the MET group of DNA methyltransferases (Jullien et al., 2012; Tirot et al., 2022). MET1 is the main CGN maintenance methyltransferase in plants, maintaining methylation of CGN sites during DNA replication (He et al., 2011; Kankel et al., 2003). MET1 is not capable of distinguishing between hemi-methylated and unmethylated CGN sites (Du et al., 2015; Song et al., 2011). Hemi-methylated DNA is, however, the preferred substrate for the DNA glycosylase base excision repair (BER) pathway that removes methylated cytosine bases and replaces them with unmethylated ones (Agius et al., 2006; Gehring et al., 2006; Gong et al., 2002; Morales-Ruiz et al., 2006; Ortega-Galisteo et al., 2008; Penterman et al., 2007). Recruitment of these components can be hypothesized to be triggered in response to elevated temperatures, resulting in CGN hyper- and hypomethylation. Taking the DNA glycosylase ROS1 as an example, it can be recruited by the increased DNA methylation (IDM) complex and acetylates histone H3 lysine 18 (H3K18Ac) around methylated cytosines (Qian et al., 2012). A similar independent recruitment mechanism has also been described recently (Liu et al., 2021).

A study in lotus (*Lotus corniculatus*) showed that methylation patterns differ between phenologically different ecotypes and suggests that these methylome differences may impact ecotype transcriptomic and phenotypic variation (Li et al., 2021). In two lotus ecotypes, gene expression patterns of 1500–2500 protein coding genes correlate with their DNA methylation pattern, of which 20% was shared between the two ecotypes. Our RNA-Seq analysis of five *F. vesca* ecotypes revealed transcriptional changes in response to temperature treatment. Increasing the temperature during sexual reproduction from 18 to 28°C caused transcriptome changes in ∼130 to ∼1200 differentially expressed genes (DEGs) in the different ecotypes. Analysis of the correlation between methylation change and altered transcription in each ecotype revealed that 4%–25% of these DEGs were also DMGs (denoted as DEDMGs). DEDMGs were statistically underrepresented, suggesting that induced changes in DNA methylation do not impact the expression of at least a subset of these DEGs.

The NOR2 and ICE2 ecotypes shared two interesting DEDMGs: a chromatin reader Tudor-domain SAWADEE homolog involved in RNA-directed DNA methylation and a small RNA-degrading nuclease (Law et al., 2011, 2013; Zhang et al., 2013). The finding that chromatin binding-related GO terms were enriched in DEDMGs in the ICE2 and NOR2 ecotypes hints that the epigenetic machinery is affected by temperature-induced methylation changes. Further studies of how chromatin status is affected by these changes could be a future direction of investigations.

We confirmed that REs has a positional effect on gene expression, as genes with REs located within 2 kb had significantly altered expression levels compared to other genes. The general effect was a reduction of expression of genes with nearby REs, in line with previous reports (Hirsch & Springer, 2017; Hollister & Gaut, 2009; Wang et al., 2013). With the exception of the NOR2 ecotype, we did not find a general correlation between differential DNA methylation and gene expression change. NOR2 displayed a significant correlation, but only when REs were located 2–5 kb from the gene and not within 2 kb or above 5 kb. We did not find an effect of REs on CGN methylation change in nearby genes. This may be explained by the fact that in plants, CHG methylation (and, to a lesser degree CHH methylation) is considered most important for transposon regulation (Wang & Baulcombe, 2020). CGN methylation may already be so high in REs that further methylation changes do not significantly influence how REs affect the expression of nearby genes.

One genome may have many epigenomes with different adaptive significance, and this epigenomic heterogeneity is a limiting factor in the study of epigenetic memory at all levels (Gallusci et al., 2023). Variable degrees of reprogramming of epigenetic marks might happen during meiosis in plants. An extreme example of differences in the maintenance of epigenetic marks during meiosis is DNA hyper- and hypomethylation induced by salt stress. This stress induces a transient maternally inherited stress memory due to a parental bias relying on the DNA (de)methylation machinery, which erases methylation primarily from male gametes (Wibowo et al., 2016). The difficulty in finding causal links between DNA methylation and gene expression is partly due to variation between individual plants, even when these plants result from selfing, as exemplified by our PCA (Figure 3A). This individual variation indicates that sexual reproduction by itself is a source of at least some of the epigenetic mark variation in the progeny, likely because recombination during meiosis creates allelic and DNA methylation variation between progenies.

AUTHOR CONTRIBUTIONS

Carl Gunnar Fossdal designed the research; Carl Gunnar Fossdal, Paul E. Grini, and Yupeng Zhang designed the analysis; Yupeng Zhang and Kathryn Mackenzie performed experiments; Yupeng Zhang, Tuomas Toivainen, Igor Yakovlev, Timo Hytönen, Paul E. Grini, and Carl Gunnar Fossdal analyzed the data; Yupeng Zhang, Timo Hytönen, Paul E. Grini, and Carl Gunnar Fossdal discussed the data; Yupeng Zhang, Paul E. Grini, and Carl Gunnar Fossdal wrote the article; Yupeng Zhang, Paal Krokene, Timo Hytönen, Paul E. Grini, and Carl Gunnar Fossdal revised the article. All authors approved the article.

ACKNOWLEDGMENTS

We would like to thank Dr. Raghuram Badmi for help with germinating *Fragaria vesca* achenes and Dr. Simeon Rossmann from NIBIO for help on R and Linux scripting. We also would like to thank Vegard Iversen, Dr. Maria Chiara Di Luca, Ingrid Johansen, and Marit

13993054, 2023, 4, Downloaded from https://onlinelibrary.wiley.com/doi/10.1111/ppl.13963 by University Of Oslo, Wiley Online Library on [12/01/2024]. See the Terms and Conditions (https://onlinelibrary.wiley.com/terms-and-conditions) on Wiley Online Library for rules of use; OA articles are governed by the applicable Creative Commons License

Langrekken from the University of Oslo for taking care of our experimental plants and Inger Heldal and Monica Skogen from NIBIO for helping in the labs. This work was supported by Norges Forskingsråd through a Toppforsk project 249958.

DATA AVAILABILITY STATEMENT

The data that support the findings of this study are openly available in Github at https://github.com/sherlock0088/FvSex.

ORCID

Yupeng Zhang https://orcid.org/0000-0001-9461-8554
Tuomas Toivainen https://orcid.org/0000-0002-2817-8121
Kathryn Mackenzie https://orcid.org/0000-0002-6246-4797
Igor Yakovlev https://orcid.org/0000-0002-2731-7433
Paal Krokene https://orcid.org/0000-0002-7205-0715
Timo Hytönen https://orcid.org/0000-0002-5231-4031
Paul E. Grini https://orcid.org/0000-0003-3898-6277
Carl Gunnar Fossdal https://orcid.org/0000-0002-7390-7864

REFERENCES

Agius, F., Kapoor, A. & Zhu, J.-K. (2006) Role of the Arabidopsis DNA glycosylase/lyase ROS1 in active DNA demethylation. *Proceedings of the National Academy of Sciences of the United States of America*, 103, 11796–11801.

Anastasiadi, D., Venney, C.J., Bernatchez, L. & Wellenreuther, M. (2021) Epigenetic inheritance and reproductive mode in plants and animals. *Trends in Ecology & Evolution*, 36, 1124–1140.

Bird, A., Taggart, M., Frommer, M., Miller, O.J. & Macleod, D. (1985) A fraction of the mouse genome that is derived from islands of non-methylated, CpG-rich DNA. *Cell*, 40, 91–99.

Borg, M., Jacob, Y., Susaki, D., LeBlanc, C., Buendía, D., Axelsson, E. et al. (2020) Targeted reprogramming of H3K27me3 resets epigenetic memory in plant paternal chromatin. *Nature Cell Biology*, 22, 621–629.

Cao, X., Aufsatz, W., Zilberman, D., Mette, M.F., Huang, M.S., Matzke, M. et al. (2003) Role of the DRM and CMT3 methyltransferases in RNA-directed DNA methylation. *Current Biology*, 13, 2212–2217.

Carneros, E., Yakovlev, I., Viejo, M., Olsen, J.E. & Fossdal, C.G. (2017) The epigenetic memory of temperature during embryogenesis modifies the expression of bud burst-related genes in Norway spruce epitypes. *Planta*, 246, 553–566.

Csorba, T., Questa, J.I., Sun, Q. & Dean, C. (2014) Antisense COOLAIR mediates the coordinated switching of chromatin states at FLC during vernalization. *Proceedings of the National Academy of Sciences of the United States of America*, 111, 16160–16165.

de Kort, H., Panis, B., Deforce, D., van Nieuwerburgh, F. & Honnay, O. (2020) Ecological divergence of wild strawberry DNA methylation patterns at distinct spatial scales. *Molecular Ecology*, 29, 4871–4881.

Du, J., Johnson, L.M., Jacobsen, S.E. & Patel, D.J. (2015) DNA methylation pathways and their crosstalk with histone methylation. *Nature Reviews. Molecular Cell Biology*, 16, 519–532.

Edger, P.P., VanBuren, R., Colle, M., Poorten, T.J., Wai, C.M., Niederhuth, C.E. et al. (2018) Single-molecule sequencing and optical mapping yields an improved genome of woodland strawberry (*Fragaria vesca*) with chromosome-scale contiguity. *GigaScience*, 7, 1–7.

Eun, C., Lorkovic, Z.J., Sasaki, T., Naumann, U., Matzke, A.J.M. & Matzke, M. (2012) Use of forward genetic screens to identify genes required for RNA-directed DNA methylation in *Arabidopsis thaliana*. *Cold Spring Harbor Symposia on Quantitative Biology*, 77, 195–204.

Finnegan, E.J. & Dennis, E.S. (2007) Vernalization-induced trimethylation of histone H3 lysine 27 at FLC is not maintained in mitotically quiescent cells. *Current Biology*, 17, 1978–1983.

Flynn, J.M., Hubley, R., Goubert, C., Rosen, J., Clark, A.G., Feschotte, C. et al. (2020) RepeatModeler2 for automated genomic discovery of transposable element families. *Proceedings of the National Academy of Sciences of the United States of America*, 117, 9451–9457.

Gallusci, P., Agius, D.R., Moschou, P.N., Dobránszki, J., Kaiserli, E. & Martinelli, F. (2023) Deep inside the epigenetic memories of stressed plants. *Trends in Plant Science*, 28, 142–153.

Gehring, M., Huh, J.H., Hsieh, T.-F., Penterman, J., Choi, Y., Harada, J.J. et al. (2006) DEMETER DNA glycosylase establishes MEDEA polycomb gene self-imprinting by allele-specific demethylation. *Cell*, 124, 495–506.

Gong, Z., Morales-Ruiz, T., Ariza, R.R., Roldán-Arjona, T., David, L. & Zhu, J.K. (2002) ROS1, a repressor of transcriptional gene silencing in Arabidopsis, encodes a DNA glycosylase/lyase. *Cell*, 111, 803–814.

Hao, Z., Lv, D., Ge, Y., Shi, J., Weijers, D., Yu, G. et al. (2020) RIdeogram: drawing SVG graphics to visualize and map genome-wide data on the idiograms. *PeerJ Computer Science*, 6, e251.

He, X.-J., Chen, T. & Zhu, J.-K. (2011) Regulation and function of DNA methylation in plants and animals. *Cell Research*, 21, 442–465.

Heo, J.B. & Sung, S. (2011) Vernalization-mediated epigenetic silencing by a long intronic noncoding RNA. *Science*, 331, 76–79.

Hirsch, C.D. & Springer, N.M. (2017) Transposable element influences on gene expression in plants. *Biochimica et Biophysica Acta, Gene Regulatory Mechanisms*, 1860, 157–165.

Hollister, J.D. & Gaut, B.S. (2009) Epigenetic silencing of transposable elements: a trade-off between reduced transposition and deleterious effects on neighboring gene expression. *Genome Research*, 19, 1419–1428.

Ingouff, M., Rademacher, S., Holec, S., Šoljić, L., Xin, N., Readshaw, A. et al. (2010) Zygotic resetting of the HISTONE 3 variant repertoire participates in epigenetic reprogramming in Arabidopsis. *Current Biology*, 20, 2137–2143.

Ji, L. & Chen, X. (2012) Regulation of small RNA stability: methylation and beyond. *Cell Research*, 22, 624–636.

Jiang, D., Gu, X. & He, Y. (2009) Establishment of the winter-annual growth habit via FRIGIDA-mediated histone methylation at flowering locus C in Arabidopsis. *Plant Cell*, 21, 1733–1746.

Jullien, P.E., Susaki, D., Yelagandula, R., Higashiyama, T. & Berger, F. (2012) DNA methylation dynamics during sexual reproduction in *Arabidopsis thaliana*. *Current Biology*, 22, 1825–1830.

Kankel, M.W., Ramsey, D.E., Stokes, T.L., Flowers, S.K., Haag, J.R., Jeddeloh, J.A. et al. (2003) Arabidopsis MET1 cytosine methyltransferase mutants. *Genetics*, 163, 1109–1122.

Kim, D.-H. & Sung, S. (2017) Vernalization-triggered Intragenic chromatin loop formation by long noncoding RNAs. *Developmental Cell*, 40, 302–312.e4.

Langmead, B. & Salzberg, S.L. (2012) Fast gapped-read alignment with bowtie 2. *Nature Methods*, 9, 357–359.

Laurent, L., Wong, E., Li, G., Huynh, T., Tsirigos, A., Ong, C.T. et al. (2010) Dynamic changes in the human methylome during differentiation. *Genome Research*, 20, 320–331.

Law, J.A., Du, J., Hale, C.J., Feng, S., Krajewski, K., Palanca, A.M.S. et al. (2013) Polymerase IV occupancy at RNA-directed DNA methylation sites requires SHH1. *Nature*, 498, 385–389.

Law, J.A. & Jacobsen, S.E. (2010) Establishing, maintaining and modifying DNA methylation patterns in plants and animals. *Nature Reviews. Genetics*, 11, 204–220.

Law, J.A., Vashisht, A.A., Wohlschlegel, J.A. & Jacobsen, S.E. (2011) SHH1, a homeodomain protein required for DNA methylation, as well as RDR2, RDM4, and chromatin remodeling factors, associate with RNA polymerase IV. *PLoS Genetics*, 7, e1002195.

Li, H., Yang, X., Wang, Q., Chen, J. & Shi, T. (2021) Distinct methylome patterns contribute to ecotypic differentiation in the growth of the storage organ of a flowering plant (sacred lotus). *Molecular Ecology*, 30, 2831–2845.

13993054, 2023, 4, Downloaded from https://onlinelibrary.wiley.com/doi/10.1111/ppl.13963 by University Of Oslo, Wiley Online Library on [12/01/2024]. See the Terms and Conditions (https://onlinelibrary.wiley.com/terms-and-conditions) on Wiley Online Library for rules of use; OA articles are governed by the applicable Creative Commons License

Lindroth, A.M., Cao, X., Jackson, J.P., Zilberman, D., McCallum, C.M., Henikoff, S. et al. (2001) Requirement of chromomethylase3 for maintenance of CpXpG methylation. *Science*, 292, 2077–2080.

Liston, A., Cronn, R. & Ashman, T.-L. (2014) Fragaria: a genus with deep historical roots and ripe for evolutionary and ecological insights. *American Journal of Botany*, 101, 1686–1699.

Liu, D., Mu, Q., Li, X., Xu, S., Li, Y. & Gu, T. (2022) The callus formation capacity of strawberry leaf explant is modulated by DNA methylation. *Horticulture Research*, 9, uhab073. Available from: https://doi.org/10.1093/hr/uhab073

Liu, P., Nie, W.-F., Xiong, X., Wang, Y., Jiang, Y., Huang, P. et al. (2021) A novel protein complex that regulates active DNA demethylation in Arabidopsis. *Journal of Integrative Plant Biology*, 63, 772–786.

Morales-Ruiz, T., Ortega-Galisteo, A.P., Ponferrada-Marín, M.I., Martínez-Macías, M.I., Ariza, R.R. & Roldán-Arjona, T. (2006) Demeter and repressor of silencing 1 encode 5-methylcytosine DNA glycosylases. *Proceedings of the National Academy of Sciences of the United States of America*, 103, 6853–6858.

Murashige, T. & Skoog, F. (1962) A revised medium for rapid growth and bio assays with tobacco tissue cultures. *Physiologia Plantarum*, 15, 473–497.

Ortega-Galisteo, A.P., Morales-Ruiz, T., Ariza, R.R. & Roldán-Arjona, T. (2008) Arabidopsis Demeter-like proteins DML2 and DML3 are required for appropriate distribution of DNA methylation marks. *Plant Molecular Biology*, 67, 671–681.

Penterman, J., Zilberman, D., Huh, J.H., Ballinger, T., Henikoff, S. & Fischer, R.L. (2007) DNA demethylation in the Arabidopsis genome. *Proceedings of the National Academy of Sciences of the United States of America*, 104, 6752–6757.

Pikaard, C.S., Haag, J.R., Pontes, O.M.F., Blevins, T. & Cocklin, R. (2012) A transcription fork model for pol IV and pol V-dependent RNA-directed DNA methylation. *Cold Spring Harbor Symposia on Quantitative Biology*, 77, 205–212.

Pontes, O., Li, C.F., Costa Nunes, P., Haag, J., Ream, T., Vitins, A. et al. (2006) The Arabidopsis chromatin-modifying nuclear siRNA pathway involves a nucleolar RNA processing center. *Cell*, 126, 79–92.

Qian, W., Miki, D., Zhang, H., Liu, Y., Zhang, X., Tang, K. et al. (2012) A histone acetyltransferase regulates active DNA demethylation in Arabidopsis. *Science*, 336, 1445–1448.

Qu, M., Li, K., Han, Y., Chen, L., Li, Z. & Han, Y. (2017) Integrated karyotyping of woodland strawberry (*Fragaria vesca*) with oligopaint FISH probes. *Cytogenetic and Genome Research*, 153, 158–164.

Samad, S., Kurokura, T., Koskela, E., Toivainen, T., Patel, V., Mouhu, K. et al. (2017) Additive QTLs on three chromosomes control flowering time in woodland strawberry (*Fragaria vesca* L.). *Horticulture Research*, 4, 17020.

Sammarco, I., Münzbergová, Z. & Latzel, V. (2022) DNA methylation can mediate local adaptation and response to climate change in the clonal plant *Fragaria vesca*: evidence from a European-scale reciprocal transplant experiment. *Frontiers in Plant Science*, 13, 827166.

Schultz, M.D., He, Y., Whitaker, J.W., Hariharan, M., Mukamel, E.A., Leung, D. et al. (2016) Human body epigenome maps reveal noncanonical DNA methylation variation. *Nature*, 530, 242.

Shulaev, V., Korban, S.S., Sosinski, B., Abbott, A.G., Aldwinckle, H.S., Folta, K.M. et al. (2008) Multiple models for Rosaceae genomics. *Plant Physiology*, 147, 985–1003.

Song, J., Rechkoblit, O., Bestor, T.H. & Patel, D.J. (2011) Structure of DNMT1-DNA complex reveals a role for autoinhibition in maintenance DNA methylation. *Science*, 331, 1036–1040.

Tao, Z., Hu, H., Luo, X., Jia, B., Du, J. & He, Y. (2019) Embryonic resetting of the parental vernalized state by two B3 domain transcription factors in Arabidopsis. *Nature Plants*, 5, 424–435.

Taudt, A., Roquis, D., Vidalis, A., Wardenaar, R., Johannes, F. & Colomé-Tatché, M. (2018) METHimpute: imputation-guided construction of complete methylomes from WGBS data. *BMC Genomics*, 19, 444.

Tavares, L., Dimitrova, E., Oxley, D., Webster, J., Poot, R., Demmers, J. et al. (2012) RYBP-PRC1 complexes mediate H2A ubiquitylation at polycomb target sites independently of PRC2 and H3K27me3. *Cell*, 148, 664–678.

Tirot, L., Bonnet, D.M.V. & Jullien, P.E. (2022) DNA methyltransferase 3 (MET3) is regulated by polycomb group complex during Arabidopsis endosperm development. *Plant Reproduction*, 35, 141–151.

Wang, X., Weigel, D. & Smith, L.M. (2013) Transposon variants and their effects on gene expression in Arabidopsis. *PLoS Genetics*, 9, e1003255.

Wang, Z. & Baulcombe, D.C. (2020) Transposon age and non-CG methylation. *Nature Communications*, 11, 1221.

Weber, M. & Schübeler, D. (2007) Genomic patterns of DNA methylation: targets and function of an epigenetic mark. *Current Opinion in Cell Biology*, 19, 273–280.

Wibowo, A., Becker, C., Durr, J., Price, J., Spaepen, S., Hilton, S. et al. (2018) Partial maintenance of organ-specific epigenetic marks during plant asexual reproduction leads to heritable phenotypic variation. *Proceedings of the National Academy of Sciences of the United States of America*, 115, E9145–E9152.

Wibowo, A., Becker, C., Marconi, G., Durr, J., Price, J., Hagmann, J. et al. (2016) Hyperosmotic stress memory in Arabidopsis is mediated by distinct epigenetically labile sites in the genome and is restricted in the male germline by DNA glycosylase activity. *eLife*, 5, e13546.

Wu, T., Hu, E., Xu, S., Chen, M., Guo, P., Dai, Z. et al. (2021) clusterProfiler 4.0: a universal enrichment tool for interpreting omics data. *Innovations*, 2, 100141.

Xu, J., Tanino, K.K., Horner, K.N. & Robinson, S.J. (2016) Quantitative trait variation is revealed in a novel hypomethylated population of woodland strawberry (*Fragaria vesca*). *BMC Plant Biology*, 16, 240.

Xu, J., Tanino, K.K. & Robinson, S.J. (2016) Stable epigenetic variants selected from an induced hypomethylated *Fragaria vesca* population. *Frontiers in Plant Science*, 7, 1768.

Yakovlev, I., Fossdal, C.G., Skrøppa, T., Olsen, J.E., Jahren, A.H. & Johnsen, Ø. (2012) An adaptive epigenetic memory in conifers with important implications for seed production. *Seed Science Research*, 22, 63–76.

Yakovlev, I.A., Asante, D.K.A., Fossdal, C.G., Partanen, J., Junttila, O. & Johnsen, O. (2008) Dehydrins expression related to timing of bud burst in Norway spruce. *Planta*, 228, 459–472.

Yakovlev, I.A., Fossdal, C.G. & Johnsen, Ø. (2010) MicroRNAs, the epigenetic memory and climatic adaptation in Norway spruce. *The New Phytologist*, 187, 1154–1169.

Yu, G., Wang, L.-G. & He, Q.-Y. (2015) ChIPseeker: an R/Bioconductor package for ChIP peak annotation, comparison and visualization. *Bioinformatics*, 31, 2382–2383.

Yu, Y., Ouyang, Y. & Yao, W. (2018) shinyCircos: an R/shiny application for interactive creation of Circos plot. *Bioinformatics*, 34, 1229–1231.

Yuan, W., Luo, X., Li, Z., Yang, W., Wang, Y., Liu, R. et al. (2016) A cis cold memory element and a trans epigenome reader mediate Polycomb silencing of FLC by vernalization in Arabidopsis. *Nature Genetics*, 48, 1527–1534.

Zeng, Z., Raffaello, T., Liu, M.-X. & Asiegbu, F.O. (2018) Co-extraction of genomic DNA & total RNA from recalcitrant woody tissues for next-generation sequencing studies. *Future Science OA*, 4, FSO309.

Zhang, H., Ma, Z.-Y., Zeng, L., Tanaka, K., Zhang, C.-J., Ma, J. et al. (2013) DTF1 is a core component of RNA-directed DNA methylation and may assist in the recruitment of pol IV. *Proceedings of the National Academy of Sciences of the United States of America*, 110, 8290–8295.

Zhang, Z., Carriero, N., Zheng, D., Karro, J., Harrison, P.M. & Gerstein, M. (2006) PseudoPipe: an automated pseudogene identification pipeline. *Bioinformatics*, 22, 1437–1439.

13993054, 2023, 4, Downloaded from https://onlinelibrary.wiley.com/doi/10.1111/ppl.13963 by University Of Oslo, Wiley Online Library on [12/01/2024]. See the Terms and Conditions (https://onlinelibrary.wiley.com/terms-and-conditions) on Wiley Online Library for rules of use; OA articles are governed by the applicable Creative Commons License

Zhao, Z., Yu, Y., Meyer, D., Wu, C. & Shen, W.-H. (2005) Prevention of early flowering by expression of FLOWERING LOCUS C requires methylation of histone H3 K36. *Nature Cell Biology*, 7, 1256–1260.

SUPPORTING INFORMATION

Additional supporting information can be found online in the Supporting Information section at the end of this article.

How to cite this article: Zhang, Y., Toivainen, T., Mackenzie, K., Yakovlev, I., Krokene, P., Hytönen, T. et al. (2023) Methylome, transcriptome, and phenotype changes induced by temperature conditions experienced during sexual reproduction in *Fragaria vesca*. *Physiologia Plantarum*, 175(4), e13963. Available from: https://doi.org/10.1111/ppl.13963

13993054, 2023, 4, Downloaded from https://onlinelibrary.wiley.com/doi/10.1111/ppl.13963 by University Of Oslo, Wiley Online Library on [12/01/2024]. See the Terms and Conditions (https://onlinelibrary.wiley.com/terms-and-conditions) on Wiley Online Library for rules of use; OA articles are governed by the applicable Creative Commons License